Signal sources in elastic light scattering by biological cells and tissues: what can elastic light scattering spectroscopy tell us?

M. Xu[a], Tao T. Wu[b], and Jianan Y. Qu[b]

[a]Department of Physics, Fairfield University, 1073 North Benson Road, Fairfield, CT 06824
[b]Department of Electronic and Computer Engineering, Hong Kong University of Science and Technology, Clear water Bay, Kowloon, Hong Kong, P. R. China
Email: mxu@mail.fairfield.edu
eequ@ust.hk

ABSTRACT

We used a unified Mie and fractal model to analyze elastic light spectroscopy of cell suspensions to obtain the size distributions of cells and nuclei, their refractive indices, and the background refractive index fluctuation inside the cell, for different types of cells, including human cervical squamous carcinoma epithelial (SiHa) cells, androgen-independent malignant rat prostate carcinoma epithelial (AT3.1) cells, non-tumorigenic fibroblast (Rat1p) cells in the plateau phase of growth, and tumorigenic fibroblast (Rat1-T1E) cells in the exponential phase of growth. Signal sources contributing to the scattering (μ_s) and reduced scattering (μ_s') coefficients for these cells of various types or at different growth stages are compared. It is shown that the contribution to μ_s from the nucleus is much more important than that from the background refractive index fluctuation. This trend is more significant with increase of the probing wavelength. On the other hand, the background refractive index fluctuation overtakes the nucleus and may even dominate in the contribution to reduced scattering. The implications of the above findings on biomedical light scattering techniques are discussed.

Keywords: elastic light scattering spectroscopy, signal sources, morphology, tissue diagnostics, epithelial cells, fibroblast cells

1. INTRODUCTION

The quest to determine signal sources in elastic light scattering by biological cells and tissues is one important ingredient in the application of light scattering techniques in biomedical applications. Light scattering of biological cells and tissues is determined by the microstructures and local refractive index variations inside the cells and tissues. Microstructures in biological tissues and mammalian cells range from organelles $0.2-0.5\mu m$ or smaller, mitochondria $1-4\mu m$ in length and $0.3-0.7\mu m$ in diameter, and nuclei $3-10\mu m$ in diameter. The refractive index variation is about $0.04-0.10$ with a background refractive index $n_0 \sim 1.35$ for soft tissues.[1] Due to the complexity of biological cells and tissues, it is a difficult and challenging task to obtain a practical light scattering model. Such a model is, however, important, as it would link the observed light scattering signals to the underlying morphological and refractive index changes and would provide a basis for use of light scattering techniques in biomedical applications. Furthermore, it could provide answers to several crucial questions such as which component of the cell dominates light scattering and whether one particular sensing approach is effective in probing the nuclear structure.

Mourant and others have conducted a series of experimental investigations on these issues.[2–6] One important finding is that inside a cell, mitochondria and other similarly sized organelles are responsible for scattering at large angles, whereas nuclei are responsible for small-angle scattering. Attempts have been made to quantify the contributions from different components inside a cell to light scattering. It is, however, difficult to assess contributions from different components inside a cell quantitatively without a workable model. Different models have been suggested in the past including Mie models,[7] discrete particle model,[1,8] a fractal model,[9] and a unified Mie and fractal model.[10,11] The finite difference time domain (FDTD) method[12,13] has also been used to study the contribution to light scattering by various structures inside the cell. The FDTD method is, however, time prohibitive for routine applications in characterizing biological cells and tissues from light scattering measurements. A practical light scattering model of cells is thus highly desireable.

Biomedical Applications of Light Scattering II, edited by Adam Wax, Vadim Backman
Proc. of SPIE Vol. 6864, 68640Y, (2008) · 1605-7422/08/$18 · doi: 10.1117/12.762368

2. SIGNAL SOURCES IN ELASTIC LIGHT SCATTERING BY BIOLOGICAL CELLS AND TISSUES: UNIFIED MIE AND FRACTAL MODEL

The unified Mie and fractal model is one such model for elastic light scattering by biological cells. In the unified mode, a biological cell is modeled as a complex composite particle (1) with the nucleus (the most important scattering center in the cell) embedded inside a bare cell host, and (2) with the presence of random fluctuation of the background refractive index inside the cell. The random fluctuation of the background refractive index is assumed to behave as a fractal based on the observed characteristics of the refractive index correlation function of tissue. [9, 14] This unified model has been validated by experimental study of the wavelength dependent angular light scattering patterns of a human cervical squamous carcinoma epithelial (SiHa) cell suspension covering the entire visible spectral range, and from forward to backward scattering angles. The analysis based on the unified model retrieved cell sizes, nucleus sizes and refractive indices of the cell and nucleus, in excellent agreement with independent measurements. [10, 11]

The signal sources of elastic light scattering by a cell arise from light scattering by (1) the bare cell, (2) the nucleus, and (3) cell background refractive index fluctuation due to the presence of mitochondria, other organelles inside the cell, and internal structures inside the nucleus. The basis to put the three parts together to describe the light scattering properties of the whole cell is the superposition rule for light scattering by a soft composite particle. [15] The bare cell is modeled as polydisperse uniform spherical scatterers. The nucleus is also modeled as polydisperse spheres whose refractive index is modified and different from the real value for the nucleus to take into account of the fact that the nucleus is embedded inside the cell and hence shadowed by the cell. The cell background refractive fluctuation is assumed to be behave as a fractal with the refractive index correlation function specified by

$$R(r) = \left\langle \delta m(0)^2 \right\rangle \int_0^{l_{\max}} \exp(-\frac{r}{l})\eta(l)dl \tag{1}$$

where $\eta(l) = \eta_0 l^{3-D_f}/l_{\max}^{4-D_f} \quad (0 \le l \le l_{\max})$ is the distribution of the correlation length l, $\left\langle \delta m(0)^2 \right\rangle$ is the squared amplitude fluctuation of the refractive index, η_0 is a dimensionless constant, and D_f is the fractal dimension.

The scattered light into direction θ with parallel or perpendicular polarization is determined by

$$I^{\parallel,\perp}(\theta) = I_0^{\parallel,\perp} N L \overline{\left|S_{\text{cell}}^{\parallel,\perp}(\theta)\right|^2}/k^2 \tag{2}$$

where $I_0^{\parallel,\perp}$ is the intensity of the incident light, N is the number density of cells in the medium, L is the path length of the probing light inside the medium, and $k = 2\pi n_{\text{bg}}/\lambda$ is the wave number with n_{bg} the refractive index of the background medium and λ the wavelength of the incident beam in vacuum. The squared scattering amplitude function $\overline{\left|S_{\text{cell}}^{\parallel,\perp}(\theta)\right|^2}$ is given by the superposition of the three components, i.e.,

$$\overline{\left|S_{\text{cell}}^{\parallel,\perp}(\theta)\right|^2} = \left|S_0^{\parallel,\perp}(\theta)\right|^2 + \left|S_n^{\parallel,\perp}(\theta)\right|^2 + \left|S_{\text{bg}}^{\parallel,\perp}(\theta)\right|^2. \tag{3}$$

Here the first two terms are due to Mie scattering by the bare cell and the nucleus, dominating light forward scattering by a cell. The polydispersity of the bare cell and that of the nucleus are assumed to follow a lognormal distribution:

$$f_i(x) \quad = \quad \frac{1}{\sqrt{2\pi}\delta_i} x^{-1} \exp\left[-\ln^2(\frac{x}{a_{m_i}})/2\delta_i^2\right], \tag{4}$$

where $i = 0, 1$ represents the bare cell and the nucleus, respectively. The refractive index of the shadowed nucleus is modified to $m_n - m_0 + 1$ where m_n and m_0 are the refractive indices for the nucleus and the bare cell, respectively. The regular Mie code is used to compute the first two terms after weighting by the lognormal size distribution Eq. (4). The third term is due to light scattering by the fluctuation in the background refractive index within the whole cell, dominating cell light scattering at other angles, and is given by,

$$\begin{aligned} \left|S_{\text{bg}}^{\perp}(\theta)\right|^2 \quad &= \quad \frac{2}{\pi}\beta^2 V k^{D_f-1} l_{\max}^{D_f-4} \int_0^{kl_{\max}} \frac{x^{6-D_f}}{[1+2(1-\cos\theta)x^2]^2} dx \\ \left|S_{\text{bg}}^{\parallel}(\theta)\right|^2 \quad &= \quad \left|S_{\text{bg}}^{\perp}(\theta)\right|^2 \cos^2\theta, \end{aligned} \tag{5}$$

	$a_{\rm cell}^{\rm eff}(\mu m)$	$\nu_{\rm cell}^{\rm eff}$	$a_{\rm nucleus}^{\rm eff}(\mu m)$	$\nu_{\rm nucleus}^{\rm eff}$	$n_{\rm cell}$	$n_{\rm nucleus}$	D_f	$l_{\rm max}(\mu m)$	β
SiHa	7.33	0.0137	5.83	0.0776	1.360	1.400	4.45	0.348	0.0093
AT3.1	7.01	0.25	3.18	0.010	1.361	1.430	3.81	1.89	0.030
Rat1p	6.43	0.0047	3.04	0.0092	1.361	1.433	4.34	1.90	0.0186
Rat1-T1E	9.26	0.0056	3.08	0.0138	1.360	1.439	4.57	1.92	0.0164

Table 1. The size distributions for the cell and the nucleus ($a_{\rm cell}^{\rm eff}$, $\nu_{\rm cell}^{\rm eff}$, $a_{\rm nucleus}^{\rm eff}$ and $\nu_{\rm nucleus}^{\rm eff}$), the refractive indices ($n_{\rm cell}$ and $n_{\rm nucleus}$) and the parameters for the background refractive index fluctuation (D_f, $l_{\rm max}$ and β) obtained by unified Mie and fractal model fitting to angular dependent elastic light scattering spectroscopy or polarized light scattering spectroscopy. SiHa: human cervical squamous carcinoma epithelial cells. AT3.1: androgen-independent malignant rat prostate carcinoma cells. Rat1p: non-tumorigenic fibroblast cells in the plateau phase of growth. Rat1-T1E: tumorigenic fibroblast cells in the exponential phase of growth.

in the fractal continuous random medium model[9] where V is the volume of the cell whose background refractive index fluctuation is characterized by a fractal dimension D_f and a cutoff correlation length $l_{\rm max}$, and $\beta = \sqrt{\langle \delta m(0)^2 \rangle \, \eta_0}$. The evaluation of Eq. (5) can be done numerically.

The light scattering characteristics of tissue depend on β and remain unchanged by scaling both $\langle \delta m(0)^2 \rangle$ and η_0 as long as their product is kept constant. Thus we can set $\eta_0 = 1$ in the unified model, yielding $\beta \equiv \sqrt{\langle \delta m(0)^2 \rangle}$ as the mean square root refractive index fluctuation and $\eta(l) \equiv l^{3-D_f}/l_{\rm max}^{4-D_f} \quad (0 \le l \le l_{\rm max})$ as the distribution for the correlation length.

3. RELATIVE IMPORTANCE OF SIGNAL SOURCES IN ELASTIC LIGHT SCATTERING BY CELLS: CASE STUDIES

The relative importance of each component for elastic light scattering by cells is one key quantity qualifying the characteristics of light scattering by cells. For example, light scattering by the cell is highly forward peaked if the nucleus dominates. The scattering power obtained from the reduced scattering coefficient wavelength dependence ($\mu_s' \propto \lambda^{-b}$) links directly to the fractal dimension ($b = D_f - 3$) if the background fluctuation dominates μ_s'. Such a connection breaks down if the background fluctuation does not dominate reduced scattering. The relative importance of each component varies with the cell type, the growth stage of the cell, and influenced by other factors including abnormal pathologies such as cancer.

We have successfully obtained the size distributions and the refractive index distribution of human cervical squamous carcinoma epithelial (SiHa) cells inside a water suspension based on the unified model fitting of angular dependent light scattering spectroscopy over the spectral range $400 - 700$ nm and a total 44 scattering angles from $1.1 - 165$ degrees.[10,11] To gain better understanding of light scattering by various types of cells, we performed the unified model analysis on reported polarized elastic light scattering spectroscopy on AT3.1 cell suspensions reported by Mourant et. al.[4] AT3.1 cells are androgen-independent malignant rat prostate carcinoma epithelial cells.

Fig. 1 displays the fitting of our model to the polarized light scattering spectroscopy of AT3.1 cell suspension. The fitting in both parallel and perpendicular polarization channels is excellent. In fitting, the refractive index of solution was assumed to be 1.334. The fitting used the Levenberg-Marquardt optimization algorithm to minimize the least squares error of the logarithmic intensities of light scattered into $5^{\rm o} - 165^{\rm o}$ in both parallel and perpendicular polarization channels. The fitting yields $a_{m_0} = 7.01\mu m$, $\delta_0 = 0.250$ and $m_0 = 1.020$ for the bare cell, $a_{m_1} = 3.18\mu m$, $\delta_1 = 0.091$, $m_1 = 1.072$ for the nucleus, and $a_{\rm max} = 1.89\mu m$, $D_f = 3.81$, and $\beta = 0.030$ for the random fluctuation of the refractive index inside the cell. The radius of cells is $6.59 \pm 3.93\mu m$, consistent with other measurements (about $7\mu m$). The radius of nuclei is $3.15 \pm 0.68\mu m$, agreeing with the size obtained for isolated nuclei.

The same technique was again used to analyze polarized elastic light scattering spectroscopy of fibroblast non-tumorigenic Rat1 cells in the plateau phase of growth (Rat1p) and tumorigenic Rat1-T1 cells in the exponential phase of growth (Rat1-T1E) reported in Ramachandran et. al.[5]

The obtained size distributions for the cell and the nucleus ($a_{\rm cell}^{\rm eff}$, $\nu_{\rm cell}^{\rm eff}$, $a_{\rm nucleus}^{\rm eff}$ and $\nu_{\rm nucleus}^{\rm eff}$), the refractive indices ($n_{\rm cell}$ and $n_{\rm nucleus}$) and the parameters for the background refractive index fluctuation (D_f, $l_{\rm max}$ and β) from the analysis with the unified Mie and fractal model for SiHa, AT3.1, Rat1p, and Rat1-T1E cells are summarized in Table 1.

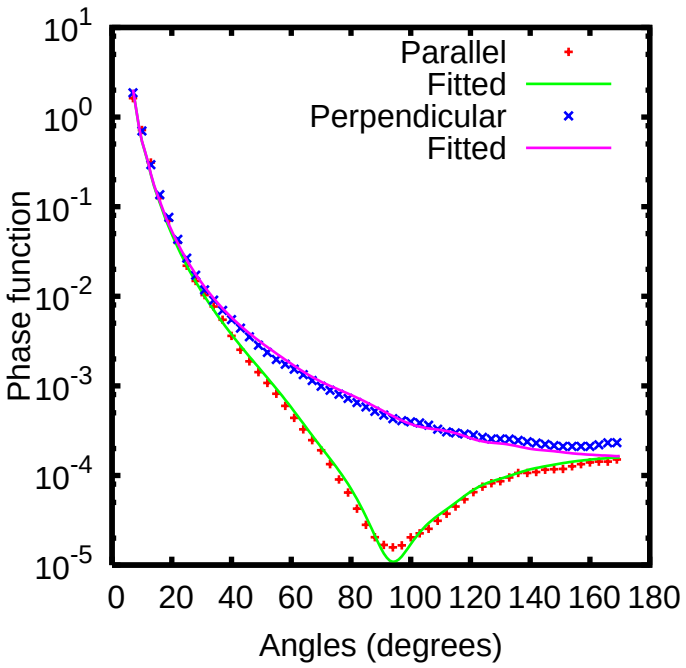

Figure 1. (Color) Fitting of the angular dependent light scattering measurements of AT3.1 cells. Both parallel and perpendicular polarized light intensities are shown.

The geometrical projection area weighted effective radius a_i^{eff}

$$a_i^{\text{eff}} = \frac{\int_0^\infty x^3 f(x)dx}{\int_0^\infty x^2 f(x)dx} = a_{m_i} \exp(5\sigma_i^2/2) \tag{6}$$

and the effective variance

$$\nu_i^{\text{eff}} = \frac{\int_0^\infty (x - a_i^{\text{eff}})^2 x^2 f(x)dx}{(a_i^{\text{eff}})^2 \int_0^\infty x^2 f(x)dx} = \exp(\sigma_i^2) - 1 \tag{7}$$

are reported in Table 1. Scatterers of different size distribution but of the same effective radius and effective variance behave alike in their light scattering properties.[16]

The size distribution of each component and their contributions to light scattering and reduced light scattering coefficients, μ_s and μ_s', for SiHa (the top row), AT3.1 (the second row), Rat1p (the third row), and Rat1-T1E (the bottom row) cells are displayed in Fig. 2. The fitting to a powerlaw (λ^{-b}) is shown for μ_s' of the unified model and its "fluctuation" component. The scattering power b should be close to $D_f - 3$ for the "fluctuation" component as expected for a fractal continuous random medium when the condition $kl_{\max} \gg 1$ is satisfied.[9] Excellent agreement is obtained for Rat1p ($b = 1.39$ and $D_f - 3 = 1.34$) and Rat1-T1E ($b = 1.59$ and $D_f - 3 = 1.57$) cells. The agreement is not as good for SiHa ($b = 1.66$ and $D_f - 3 = 1.45$) and AT3.1 ($b = 0.97$ and $D_f - 3 = 0.81$) cells due to the small cutoff correlation length $l_{\max}$ in SiHa cells and the low diffraction dimension in AT3.1 cells.

The relation $b = D_f - 3$ approximately holds for the reduced scattering coefficient of the whole cell in the case of SiHa cells ($b = 1.36$ and $D_f = 1.45$). However, it breaks down for the reduced scattering coefficient of the whole cell of AT3.1, Rat1p and Rat1-T1E cells where light scattering from the nucleus plays a role as important as the background fluctuation in μ_s'.

Fig. 3 displays the relative importance of the contribution from the nucleus versus that from the cell background refractive index fluctuation. The contribution to μ_s from the nucleus is always more important than that from the background fluctuation, independent of cell types or growth stages investigated here. This trend is more significant with increase of the probing wavelength. On the other hand, the background fluctuation, in general, overtakes the nucleus in its contribution to μ_s'. In particular, for SiHa cells, the reduced scattering is almost completely determined by the background fluctuation.

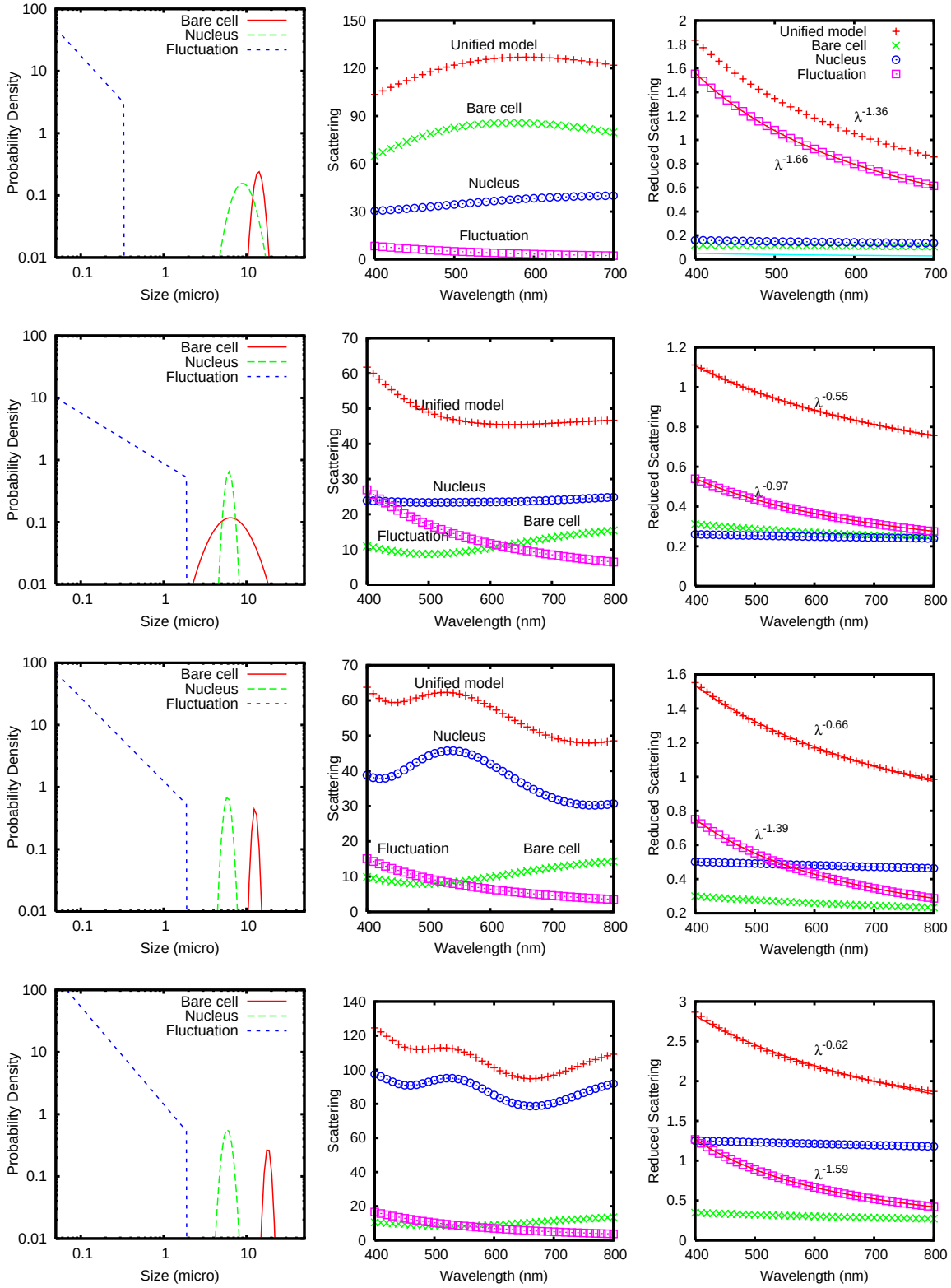

Figure 2. (Color) The size distribution of each component and their contributions to light scattering and reduced light scattering coefficients, μ_s and μ_s', for SiHa (the top row), AT3.1 (the second row), Rat1p (the third row), and Rat1-T1E (the bottom row) cells. The fitting to a powerlaw is shown for μ_s' for the unified model and its "fluctuation" component.

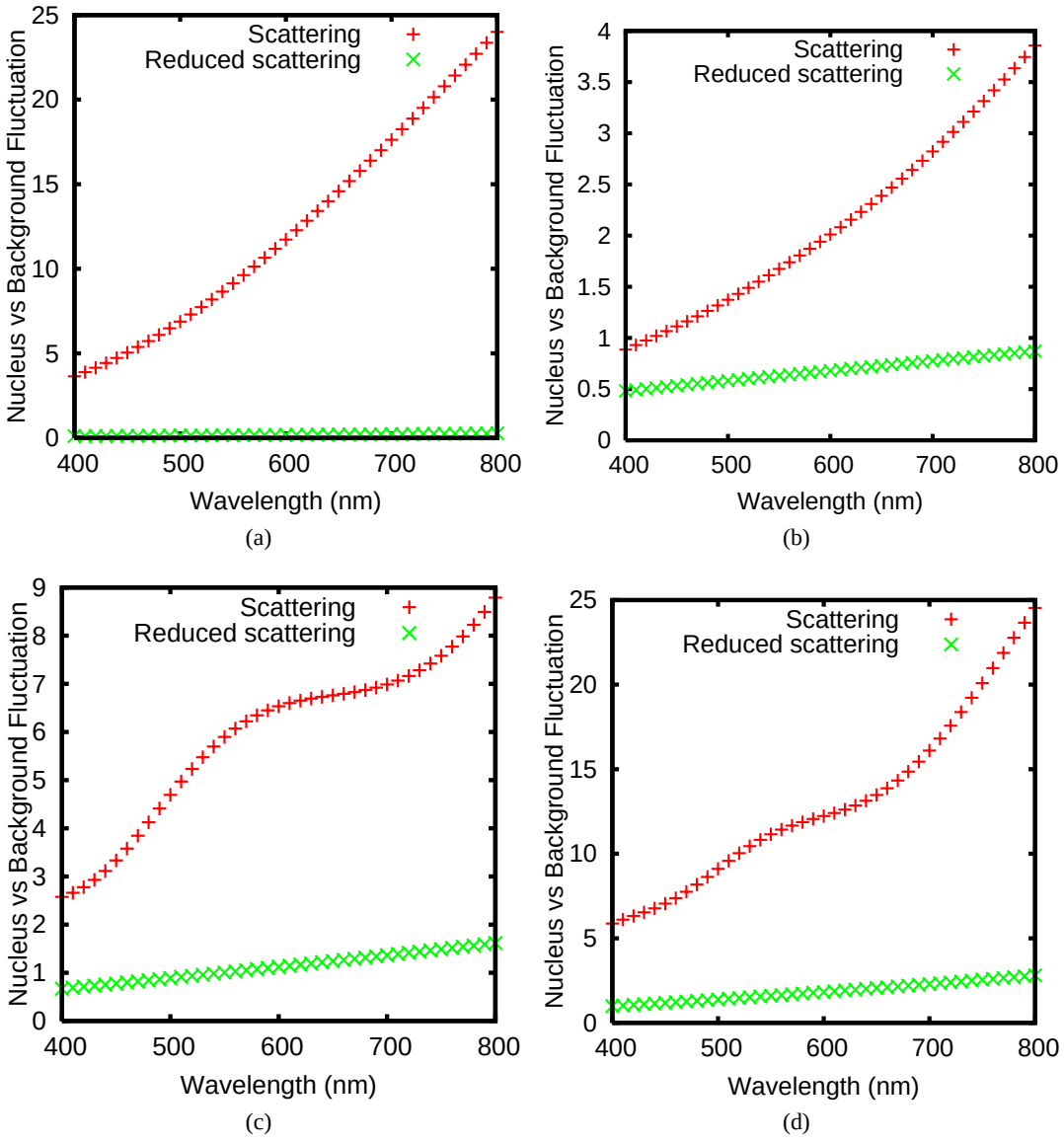

Figure 3. (Color) The relative importance of the contribution from the nucleus versus that from the cell background refractive index fluctuation. The ratios of their contributions to μ_s and μ_s' are plotted for (a) SiHa, (b) AT3.1, (c) Rat1p, and (d) Rat1-T1E cells.

4. DISCUSSION AND CONCLUSION

From the above analysis, signal sources in elastic light scattering by a biological cell may arise from the bare cell, the nucleus, and the cell background random fluctuation in the refractive index owing to the presence of mitochondria, other organelles and structures inside the nucleus. The importance of each component varies with the type of cell. Difference in the growth stage or pathology status will also have influence on the detail of light scattering characteristics of cells.

The mean refractive index of the cell cytoplasm is within $1.360 - 1.361$ for all these different types of cells investigated here. The mean refractive index of the nucleus varies much more than that of the cytoplasm. The value of the mean refractive index for the nucleus can be as large as 1.439 for Rat1-T1E fibroblast cells and as low as 1.400 for SiHa epithelial cells. The fractal dimension of the background fluctuation (D_f) is observed to be smaller for carcinoma cells than normal cells.

Reduced scattering coefficient μ_s' is commonly measured in optical tissue sensing as it is much easier to measure than the scattering coefficient μ_s. The scattering power b of the reduced scattering wavelength dependence relates to the fractal dimension D_f of the background refractive index fluctuation owing to a fractal-like background refractive index correlation inside tissue.[9] The simple expression $b = D_f - 3$ is approximately true when the background refractive index fluctuation dominates μ_s', as in the case of SiHa epithelial cells. When the contribution to μ_s' from the nucleus is important, the scattering power b becomes much smaller than $D_f - 3$. The simple $b = D_f - 3$ rule breaks down. This suggests one has to be careful in interpreting the scattering power. The value of b reflects morphology and refractive index of both the nucleus and the background fluctuation. Cells of different types differ significantly in which component plays the leading role in determination of the reduced scattering coefficient. This means one particular technique effective for one kind of cells may be inappropriate for another type of cells. Cell or tissue models need to be carefully assessed in validating any light scattering technique for tissue diagnostics.

It is also evident that the probing of the scattering coefficient rather than the reduced scattering coefficient may provide a more direct handle to the nuclear structure inside the cell as light scattering coefficient is always dominated by the nuclear contribution for epithelial and fibroblast cells investigated here. Optical sensing techniques able to probe μ_s directly is worth serious investigation, in particular, for cancer detection.

ACKNOWLEDGMENTS

This work is supported by Cottrel College Science Award.

REFERENCES

1. J. M. Schmitt and G. Kumar, "Optical scattering properties of soft tissue: A discrete particle model," *Appl. Opt.* **37**, pp. 2788–2797, May 1998.
2. J. R. Mourant, J. P. Freyer, A. H. Hielscher, A. A. Eick, D. Shen, and T. M. Johnson, "Mechanisms of light scattering from biological cells relevant to noninvasive optical-tissue diagnostics," *Appl. Opt.* **37**, pp. 3586–3593, June 1998.
3. J. R. Mourant, M. Canpolat, C. Brocker, O. Esponda-Ramos, T. M. Johnson, A. Matanock, K. Stetter, and J. P. Freyer, "Light scattering from cells: the contribution of the nucleus and the effects of proliferative status," *J. Biomed. Opt.* **5**, pp. 131–137, 2000.
4. J. R. Mourant, T. M. Johnson, S. Carpenter, A. Guerra, T. Aida, and J. P. Freyer, "Polarized angular dependent spectroscopy of epithelial cells and epithelial cell nuclei to determine the size scale of scattering structures.," *J Biomed Opt* **7**, pp. 378–387, Jul 2002.
5. J. Ramachandran, T. M. Powers, S. Carpenter, A. Garcia-Lopez, J. P. Freyer, and J. R. Mourant, "Light scattering and microarchitectural differences between tumorigenic and non-tumorigenic cell models of tissue," *Opt. Express* **15**, pp. 4039–4053, 2007.
6. T. T. Wu and J. Y. Qu, "Assessment of the relative contribution of cellular components to the acetowhitening effect in cell cultures and suspensions using elastic light-scattering spectroscopy," *Appl. Opt.* **21**, pp. 4834–4842, 2007.
7. A. Brunsting and P. F. Mullaney, "Light scattering from coated spheres: model for biological cells," *Appl. Opt.* **11**, pp. 675–680, 1972.
8. R. K. Wang, "Modeling optical properties of soft tissue by fractal distribution of scatterers," *J. Mod. Opt.* **47**, pp. 103–120, 2000.

9. M. Xu and R. R. Alfano, "Fractal mechanisms of light scattering in biological tissue and cells," *Opt. Lett.* **30**, pp. 3051–3053, 2005.
10. T. T. Wu, J. Y. Qu, and M. Xu, "Unified Mie and fractal scattering by biological cells and subcellular structures," *Opt. Lett.* **32**, pp. 2324–2326, 2007.
11. M. Xu, T. T. Wu, and J. Y. Qu, "Unified mie and fractal scattering by cells and experimental study on application in optical characterization of cellular and subcellular structures," *J. Biomed. Opt.* , 2007. (in press).
12. A. Taflove, *Computational electrodynamics: The finite difference time-domain method*, Artech House, London, 1995.
13. R. Drezek, A. Dunn, and R. Richards-Kortum, "A pulsed finite-difference time-domain (FDTD) method for calculating light scattering from biological cells over broad wavelength ranges," *Opt. Express* **6**, pp. 147–157, 2000.
14. J. M. Schmitt and G. Kumar, "Turbulent nature of refractive-index variations in biological tissue," *Opt. Lett.* **21**, pp. 1310–1312, 1996.
15. M. Xu, "Superposition rule for light scattering by a composite particle," *Opt. Lett.* **31**, pp. 3223–3225, 2006.
16. M. I. Mishchenko, L. D. Travis, and A. A. Lacis, *Scattering, absorption and emission of light by small particles*, Cambridge University Press, 2002.